

# Novel Imaging Method to Quantify Stratum Corneum in Dermatopharmacokinetic Studies: Proof-of-Concept with Acyclovir Formulations

Lisa M. Russell · Richard H. Guy

Received: 5 May 2012 / Accepted: 5 July 2012 / Published online: 19 July 2012  
© Springer Science+Business Media, LLC 2012

## ABSTRACT

**Purpose** Tape-stripping the stratum corneum (SC) is used in the assessment of dermatopharmacokinetics (DPK). The amount of SC per tape can be determined gravimetrically, but a novel imaging method offers advantages in terms of sensitivity, reproducibility, precision, stability and speed. High-resolution images, acquired under controlled conditions, are analysed in terms of pixel greyscale values and distributions, and their usefulness in DPK studies is demonstrated in this study using acyclovir.

**Methods** At all tape-stripped sites, the SC amount per tape was measured gravimetrically and by imaging. In a first series of experiments, untreated sites were stripped to determine total SC thickness. Subsequently, post-application of two acyclovir creams, drug-permeation profiles were constructed.

**Results** The greyscale values from the imaging data can be used directly to estimate total SC thickness and DPK parameters. The results compared favourably with the traditional weighing method. The concentration of drug on each tape, as a function of the relative position within the SC, permitted diffusivity and partitioning parameters characterising the penetration of acyclovir to be derived.

**Conclusion** The new imaging approach offers a sensitive, reproducible, precise, and rapid technique to quantify the relative SC amount removed on tape-strips, and facilitates the acquisition of DPK data.

**KEY WORDS** dermatopharmacokinetics · imaging · stratum corneum · tape stripping

## ABBREVIATIONS

ACV	acyclovir
$ANG_i$	absolute normalised SC greyscale on tape $i$
$ANT_i$	absolute normalised SC thickness on tape $i$
B	baseline correction factor for non-linear model using cumulative thickness
$B_g$	baseline correction factor for non-linear model using cumulative greyscale
$C_g$	drug concentration at depth $g$ , within SC, as measured by cumulative integrated pixel density
$C_{max}$	maximum drug concentration achieved in SC
CV	coefficient of variation
$C_v$	drug concentration in the vehicle
$C_x$	drug concentration at depth $x$ , within SC, as measured gravimetrically
$D/H^2$	drug's diffusivity parameter in SC
DPK	dermatopharmacokinetics
$D_w$	diffusivity of water in SC
G	total SC thickness estimated by greyscale integrated pixel density
G	cumulative integrated pixel density of SC removed by tape stripping
$g/G$	relative depth reached within SC measured by integrated pixel density of SC per tape
H	cumulative thickness of SC removed by tape stripping
H	total SC thickness estimated gravimetrically
$h/H$	relative depth reached within the SC measured gravimetrically
$K_g$	SC-vehicle partition coefficient of drug determined from drug concentration measured by cumulative integrated pixel density
$K_m$	SC-vehicle partition coefficient of drug determined from drug concentration measured gravimetrically
$k_p$	permeability coefficient of drug through SC

L. M. Russell · R. H. Guy (✉)  
Department of Pharmacy and Pharmacology, University of Bath  
Claverton Down  
Bath BA2 7AY, UK  
e-mail: r.h.guy@bath.ac.uk

$K_{SC/VE}$	SC-viable epidermis partition coefficient of water
$R_g$	average concentration of drug in SC quantified by greyscale integrated pixel density
$R_m$	average concentration of drug in SC quantified gravimetrically
$r_s$	Spearman's correlation coefficient (non-parametric correlation)
SC	stratum corneum
SER	standard error of regression
TEWL	transepidermal water loss
$TEWL_0$	initial TEWL measured before tape stripping
$\Delta C_w$	concentration gradient of water across the SC

## INTRODUCTION

Dermatopharmacokinetics (DPK) permits the rate and extent of drug permeation through the skin to be determined by analyzing the active compound in stratum corneum (SC) layers, which are progressively removed by tape-stripping (1–11). When the drug concentration on each tape is determined individually, penetration profiles may be derived, as a function of depth within the SC (and, to facilitate comparison between the results of different experiments, these depths are expressed relative to the total SC thickness, which is measured separately).

The drug concentration profiles can be fitted to an appropriate solution of Fick's second law of diffusion, to derive the SC-vehicle partition coefficient and a measure of the drug's diffusivity in the SC (12–20). These parameters may then be compared for different formulations (14,17,19,20). The amount of SC on each tape is required (a) to express the drug mass measured per tape as a concentration (in terms of a SC 'volume'); (b) to measure the depth reached within the SC; and (c) to measure, at a separate site, the total SC thickness so that the depth reached may be expressed relative to this value at each site tested in each subject.

Traditionally, weighing tapes before and after stripping has been used to estimate the mass of SC removed per tape (1). The latter is then converted to SC thickness using the known the area and SC density ( $\sim 1 \text{ g/cm}^3$  (21)). At an adjacent, untreated site, stripping is performed with concomitant TEWL measurements, to derive an estimate for the total SC thickness (22,23).

Recently (24), a novel imaging method has been developed to quantify SC on tape-strips and shown to be more precise and sensitive than the gravimetric approach, with a higher signal-to-noise ratio. A high-resolution image of each tape is acquired under controlled lighting conditions, and the individual pixels provide an associated greyscale value, which may be measured and analysed. The mean greyscale value per tape multiplied by the strip area provides a relative measure (the integrated pixel density) of SC on the tape.

In this paper, an initial series of experiments determined cumulative integrated pixel densities ( $g$ ) and, with concomitant transepidermal water loss (TEWL) measurements, were input directly into a non-linear model (23) to estimate total SC thickness ( $G$ ) in human volunteers. Subsequently, the cumulative integrated pixel density on each tape strip was used to provide proof-of-concept for the greyscale measure of SC amount per tape and to derive dermatopharmacokinetic profiles for two topical acyclovir (ACV) cream formulations.

## MATERIALS AND METHODS

An initial set of experiments was performed to determine whether greyscale values could be used to estimate total SC thickness; comparisons were made with gravimetric measurements. Subsequently, a proof-of-concept study examined the use of greyscale values in existing dermatopharmacokinetic models to compare two acyclovir formulations; validation of the approach involved parallel assessment of concentration profiles with the traditional gravimetric technique for SC quantification.

### Subjects

Healthy volunteers, with no history of dermatological disease, participated in the study. Ethical approval was granted by the Salisbury Local Research Ethics Committee; the Declaration of Helsinki protocols were followed, and written informed consent was obtained from all volunteers. Participants refrained from using any topical products on the test area on the day of the experiments.

### Tape Stripping

$2 \times 3 \text{ cm}^2$  tapes were cut from Scotch Book tape 845 (3M, St. Paul, MN) and stored overnight in covered trays.

Prior to any tape stripping experiment, two light "pre-tapes" were applied and discarded. A plastic template was used to delimit a constant area of skin ( $1.5 \times 1.5 \text{ cm}^2$ ). This template had an outline marked on its underside of  $2 \times 3 \text{ cm}^2$  to ensure that the tapes were always placed in the same position.

Initial transepidermal water loss (TEWL) measurements were taken, until stable, with a closed-chamber evaporimeter (Biox Aquaflux AF102, Biox Systems, Ltd., London, UK; probe applied for at least 60s, TEWL was recorded once the mean of 10 successive measurements had a CV < 1%). A pre-weighed tape (see below) ( $2 \times 3 \text{ cm}^2$ ) was positioned over the template. Adhesion was ensured with six passes over the tape with a weighted roller before swift removal. TEWL was re-measured. This sequence of tape strip and TEWL measurement was continued until the rate

of water loss had increased to 4–5 times the control, pre-stripping value.

### Techniques to Quantify SC on Tape Strips

The SC amount on each tape was determined by both gravimetric and imaging methods.

#### Weighing Method

Tapes were cut and stored (covered) for 12 h in ambient conditions. Each blank tape was discharged of static electricity (R50 discharging bar with ES50 power supply from Eltex Electrostatik GmbH, Weil am Rhein, Germany), weighed on a microbalance (SE-2F, precision 0.1 µg; Sartorius AG, Goettingen, Germany) and then stored (maximum 24 h) before being used for tape stripping. Following tape stripping, all tapes were again discharged of static electricity and reweighed. The mass difference between the two allowed the mass of SC on each tape to be calculated.

To correct for any variations in environmental conditions, and the change in mass that may occur over time, 3–5 blank tapes were weighed at the same time as those used for stripping. The change in mass of these blank tapes was used to correct the calculated mass of SC on each tape used in the experiments.

Knowing the mass of SC on the tape, the area, and the density of SC ( $\sim 1 \text{ g/cm}^3$ ) (21), the thickness of SC on each tape could be calculated, and hence the cumulative SC thickness removed derived.

#### Imaging Method

The procedure followed the steps outlined above but, after the second weighing, the tapes were mounted onto slides before being photographed under controlled lighting conditions using a Coolscan V ED (Nikon UK Limited, Kingston upon Thames, UK) slide scanner. Image resolution was 4000 pixels per inch. The scanner was set to positive scan in the greyscale colour space of 14-bit depth, with no transformations or camera adjustments.

Cropped images,  $2213 \times 2203$  pixels (approximately  $1.4 \times 1.4 \text{ cm}^2$ ; 9822 KB each) were taken and then analysed with ImageJ (Rasband, W.S., U. S. National Institutes of Health, Bethesda, Maryland, USA; freeware from <http://rsb.info.nih.gov/ij/>). A scale of 159.07 pixels/mm was applied by measuring the full length of one side of the image. During image analysis, the 16-bit greyscale value of each of the 4875239 pixels in the image is found, in the range from 0 (black) to 64608 (white). The mean corrected greyscale value across all pixels was derived by subtracting from the mean greyscale value for a blank tape (64355); hence, large corrected mean greyscale values correspond to dark images,

and more stratum corneum. The mean greyscale value of each tape was multiplied by the tape strip area ( $195 \text{ mm}^2$  for all tapes in this study) to derive the integrated pixel density, a relative measure of SC per tape.

### Modeling and Statistics

All non-linear modeling was performed in WinNonLin® (software version 5.1, Pharsight Corporation, Mountain View, CA) using ASCII user-defined models. In all cases, no data points were excluded, uniform weighting was applied, and no bounds were used.

All statistical tests were performed, and graphs produced, with GraphPad Prism® (version 4.00 for Windows, GraphPad Software, San Diego, CA).

### Initial Experiments to Estimate Total SC Thickness

#### Subjects

A total of 25 sites from eight volunteers (2 male, 6 female, age range 23–37 years) were examined over a period of 14 months. The experiment generated a total of 388 tape strips, a variable number of which was obtained at each site, as the criterion for terminating the tape-stripping process was that TEWL had reached 4–5 times the initial value for that site. Repeat participation using the same arm was treated as a separate measurement and was delayed by at least 1 month, which is sufficient for barrier regeneration (25–27).

#### Non-linear Modeling

To determine the SC thickness of each volunteer, tape stripping was performed on an untreated site with TEWL measurements taken before and after each tape strip. The sequence was repeated until the TEWL value was 4–5 times its initial value (i.e., usually  $60\text{--}80 \text{ g.m}^{-2} \text{ h}^{-1}$ ). As mentioned before, the SC amount on each tape was determined by both gravimetric and imaging methods.

The total SC thickness,  $H$  or  $G$ , was estimated from the baseline-corrected non-linear model (23) using either the SC thickness (Eq. 1) or integrated pixel densities (Eq. 2), respectively:

$$TEWL = B + \frac{K_{SC/VE} \cdot D_w \cdot \Delta C}{H - h} \quad (1)$$

$$TEWL = B_g + \frac{(K_{SC/VE} \cdot D_w \cdot \Delta C)_g}{G - g} \quad (2)$$

In Eq. 1, the thickness of the SC removed ( $h$ ), is determined gravimetrically. The change in TEWL as a function of thickness of SC stripped is fitted to the equation to obtain

values of (a) the SC thickness ( $H$ ), (b) the product of the SC- viable epidermal partition coefficient of water ( $K_{SC/VE}$ ), its diffusivity in the barrier ( $D_w$ ), and the concentration gradient ( $\Delta C$ ) of water across the membrane, and (c) the baseline correction factor ( $B$ ).

In Eq. 2, the SC removed by each strip is assessed by the imaging method. The cumulative integrated pixel density ( $g$ ) for each tape is used in this expression to yield the total SC thickness ( $G$ ) and, once again, values for  $D_w \cdot K_{SC/VE} \cdot \Delta C$  and  $B$ . Values derived from this model are denoted with subscript 'g'.

To compare easily whether the plots of TEWL against either cumulative thickness or cumulative integrated pixel density, and the resultant fits to Eq. 1 or Eq. 2, respectively, are equivalent, the profiles were normalised by dividing each individual cumulative value by the total SC thickness ( $H$  or  $G$  respectively). The following mathematically equivalent models are thereby deduced from Eqs. 1 and 2, respectively:

$$TEWL = B + \frac{(K_{SC/VE} \cdot D_w \cdot \Delta C)/H}{1 - h/H} \quad (3)$$

$$TEWL = B_g + \frac{(K_{SC/VE} \cdot D_w \cdot \Delta C)_g/G}{1 - g/G} \quad (4)$$

In the same way, total SC thickness was determined for the sites used in the formulation DPK study to normalize the concentration profiles obtained in the different volunteers.

$h/H$  with  $g/G$  values from a particular site are cumulative, and thus co-dependent. To assess whether the gravimetric and imaging methods produce comparable values for *each tape* individually, the absolute normalised SC thickness on tape  $i$  ( $ANT_i$ ) and the absolute normalised integrated pixel density determined for tape  $i$  ( $ANG_i$ ) were calculated with Eqs. 5 and 6, respectively:

$$ANT_i = (h/H)_i - (h/H)_{i-1} \quad (5)$$

$$ANG_i = (g/G)_i - (g/G)_{i-1} \quad (6)$$

## Determination of Drug Concentration Profiles

### Subjects and Formulations

Two healthy female volunteers (both 30 years old), with no history of dermatological disease, participated in this study.

The DPK of two 5% *w/w* acyclovir cream formulations, Zovirax (GlaxoSmithKline plc, Brentford, UK), and a generic product (Pliva Pharma, Ltd, Petersfield, UK), were compared. Five skin sites were examined for each volunteer: 2 sites for each of the two formulations, and one site at which SC thickness was determined.

400  $\mu$ L (HandyStep® volume dispenser, Brand GMBH & Co. KG, Wertheim Germany) of each formulation was spread over a demarcated area ( $2 \times 2$  cm<sup>2</sup>, foam template, No.1772, 3M United Kingdom PLC, Bracknell, UK), covered with plastic to provide occlusive conditions and left in place for 30 min. This corresponds to an infinite dose, chosen such that (i) no significant depletion of drug occurs over the course of the experiment, and (ii) the DPK models based on Fick's 2nd law apply. At the end of the application, the site was carefully cleaned with 3 wipes each of a dry tissue, and an alcohol wipe (Klervicide, Shield Medicare Ltd, Farnham, UK), and allowed to dry for 5 min. This cleaning procedure was considered sufficient to remove any excess formulation, which would otherwise lead to an artificially large concentration of acyclovir being detected in initial tape strips. A plastic template delimiting an area of  $1.5 \times 1.5$  cm<sup>2</sup> was centered over the application area and tape stripping was performed.

### Acyclovir Extraction and Analysis

After tape stripping, the amount of SC per tape was measured by gravimetric and imaging methods (see above). Subsequently, tapes were cut from the slide holders, and extracted overnight in 1 ml of distilled water (recoveries  $\geq 95\%$ ). Samples were filtered (Chronus® 0.45  $\mu$ m nylon filters, SMI-LabHut Ltd, Maisemore, UK) before HPLC analysis (PG80 pump, ASI-100 autosampler, TCC-100 column oven, PDA-100 UV lamp from Dionex Corporation Sunnyvale, California, USA) using a 15 cm Acclaim 120 column (C18, 5  $\mu$ m, 120 Å) at 25°C and a mobile phase of (by volume) 0.5% acetic acid, 5% methanol, and 94.5% water (pH 2.97) running at 1 mL/min. The drug was detected at 254 nm; no interference with formulation excipients or skin was observed. The LOQ and LOD of the assay were  $0.049 \pm 0.004$  and  $0.016 \pm 0.001$   $\mu$ g/mL, respectively.

A linear calibration curve was derived using standard solutions of acyclovir (Sequoia Research Products Ltd., Pangbourne, United Kingdom) in distilled water, over the concentration range 0.024-1.96  $\mu$ g/mL.

### Dermatopharmacokinetic Profiles

Two concentration profiles were constructed; one based on SC depth determined gravimetrically, the other according to the integrated pixel density.

For the 'mass-derived' concentration profiles, the concentration of drug at a particular depth ( $C_x$ ) can be expressed in terms of ACV mass per mass of SC on the tape; however, when the SC is quantified by imaging, the ACV mass is divided by the corresponding mean greyscale value, expressed as  $C_g$ . To allow the two approaches to be directly compared, therefore, a normalisation procedure is required and this is achieved by dividing the two sets of concentration

data, respectively, by the average concentration of drug in the SC as determined by mass ( $R_m$ ) and the average concentration of drug in the SC as determined by imaging ( $R_g$ ) using Eqs. 7 and 8. Estimates of the average concentration of drug in the SC can also be found from the area under the concentration profiles:

$$R_m = \frac{\text{Total ACV mass from all tapes } (\mu\text{g})}{\text{Total SC mass from all tapes } (\text{mg})} \approx \int_0^1 C_x d(h/H) \quad (7)$$

$$R_g = \frac{\text{Total ACV mass from all tapes } (\mu\text{g})}{\text{Total SC mean greyscale value from all tapes}} \approx \int_0^1 C_x d(g/G) \quad (8)$$

The normalised concentration of drug ( $C_x/R_m$  or  $C_g/R_g$ ), as a function of time ( $t$ ) and of position ( $h$  or  $g$ ) in the SC of total thickness ( $H$  or  $G$ ), may be expressed by the following solutions of Fick's 2nd law of diffusion:

$$\frac{C_x}{R_m} = \frac{K_m}{R_m} \cdot C_v \left[ (1 - h/H) - \frac{2}{\pi} \sum_{n=1}^{10} \frac{1}{n} \sin(n\pi \cdot \frac{h}{H}) \exp(-n^2 \cdot \pi^2 \cdot (D/H^2) \cdot t) \right] \quad (9)$$

$$\frac{C_g}{R_g} = \frac{K_g}{R_g} \cdot C_v \left[ (1 - g/G) - \frac{2}{\pi} \sum_{n=1}^{10} \frac{1}{n} \sin(n\pi \cdot \frac{g}{G}) \exp(-n^2 \cdot \pi^2 \cdot (D/H^2) \cdot t) \right] \quad (10)$$

where  $C_v$  is the drug concentration in the vehicle. Two key DPK parameters may be estimated by fitting the experimental data to Eqs. 9 and 10: specifically, (i) a normalised estimate of the drug's SC-vehicle partition coefficient ( $K_m/R_m$  or  $K_g/R_g$  for the mass and greyscale measurements, respectively), and (ii) its characteristic diffusion parameter through the SC ( $D/H^2$ , which has units of a 1st-order rate constant,  $[\text{time}]^{-1}$ ). Equations 9 and 10 require the following boundary conditions: (a) that an infinite dose is applied; (b) that the SC is initially drug-free; (c) that the barrier is homogeneous in its properties; and (d) that the viable epidermis provides a perfect sink for permeating drug.

## RESULTS

### Estimating Total SC Thickness

For each tape stripping site, two estimates of total SC thickness,  $H$  and  $G$ , were determined, respectively, from the change in TEWL as a function of (a) the cumulative

thickness of SC (measured gravimetrically and fitted to Eq. 1), and (b) the cumulative greyscale value (measured by the imaging method and fitted to Eq. 2). Representative data and the corresponding fits of the non-linear models for one subject are shown in Figs. 1a and b.

Figure 2 shows the significant correlation between the  $H$  and  $G$  estimates over the 25 sites investigated ( $p < 0.0001$ , 2-tailed Gaussian approximation, Spearman correlation coefficient,  $r_s = 0.80$ ). SC thicknesses measured with the gravimetric method varied from 8.9 to 22.6  $\mu\text{m}$ , with a mean ( $\pm$  standard deviation) of 13.6 ( $\pm$  4.0)  $\mu\text{m}$ , a value in good agreement with previous findings (13).

The normalised values of  $(D_w \cdot K_{SC/VE} \cdot \Delta C/H)$  and  $(D_w \cdot K_{SC/VE} \cdot \Delta C)_g/G$  over all 25 data sets were remarkably similar: 7.38 ( $\pm$  2.27) and 7.47 ( $\pm$  2.49), respectively (Fig. 3), and significantly (and positively) correlated:  $\alpha = 0.05$ , Spearman correlation coefficient = 0.93.

Before any stripping begins,  $h$  and  $g$  are zero, and Eqs. 1 and 2 predict linear relationships between  $[\text{TEWL}_0 - D_w \cdot K_{SC/VE} \cdot \Delta C/H]$  and  $B$ , and between  $[\text{TEWL}_0 - (D_w \cdot K_{SC/VE} \cdot \Delta C)_g/G]$  and  $B_g$ , respectively. The resulting Spearman correlation coefficients of 0.91 and 0.94 confirm that the non-linear models fit the data well.

### Intra-subject Variability

Typically, when using tape-stripping to evaluate bioequivalence between topical formulations, SC thickness is determined at one skin site to normalise the DPK data obtained at adjacent sites (1). This approach assumes, of course, that SC thickness is similar, on the whole, across the ventral forearm. To validate this hypothesis, the SC thickness of 4 volunteers on 3–5 adjacent skin sites, on the same arm, on the same day, was determined using results from both gravimetric (Eq. 1) and imaging (Eq. 2) experiments (Table I).

Comparing the relative standard deviation (RSD) values for the two models, in Subjects 1, 2 and 4, the estimate for  $G$  has a lower RSD than the corresponding  $H$  estimate. It is also interesting to note that the  $G$  estimates from the different sites always had a RSD  $< 10\%$ , whereas the  $H$  estimates for Subjects 1, 2 and 4 have RSD  $> 10\%$ . These data suggest that the  $G$  estimate of SC thickness (from Eq. 2) is less variable than that for  $H$  (from Eq. 1).

### Comparison of Normalised Profiles

To facilitate comparison of the data from the the gravimetric and imaging methods, the cumulative thickness values were divided by  $H$  (yielding  $h/H$  values), and the cumulative integrated pixel densities were divided by  $G$  (producing  $g/G$  values), as explained above. The results and the fits may then be superimposed (see Fig. 1c).



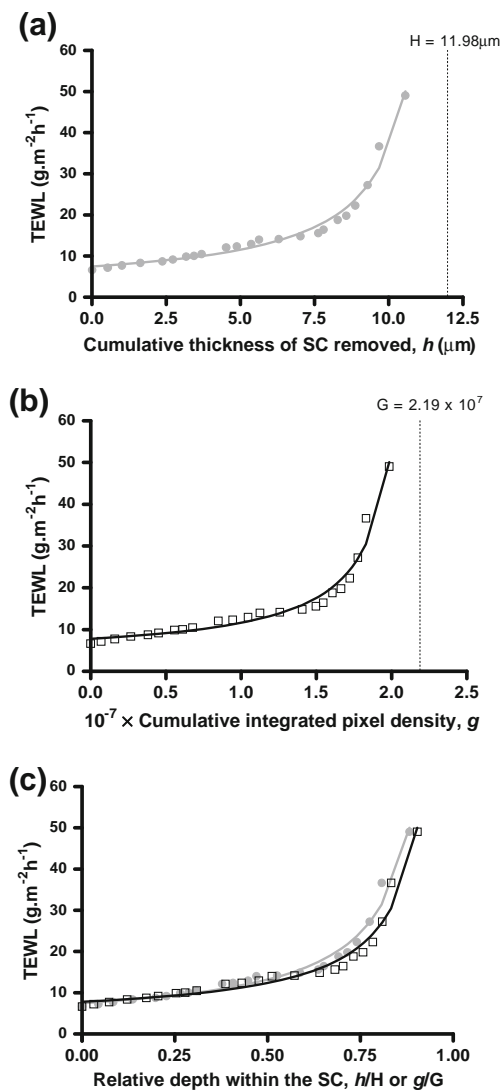


**Fig. 1** Representative TEWL measurements as a function of cumulative thickness and cumulative integrated pixel density values for one subject. **(a)** TEWL vs. cumulative thickness of SC removed (experimental data points (●) and fit to Eq. 1 (—)); estimated  $H=12.0 \mu\text{m}$ . **(b)** TEWL vs. cumulative integrated pixel density of SC removed (experimental data points (□) and fit to Eq. 2 (—)); estimated  $G=2.2 \times 10^7$ . **(c)** Superimposed, normalised profiles: (a) TEWL vs. normalised cumulative thickness,  $h/H$  (●) and the resultant fit to Equation (—); (b) TEWL vs. normalised cumulative integrated pixel density,  $g/G$  (□) and the resultant fit to Eq. 4 (—).

While the absolute SC thickness (expressed as either  $H$  or  $G$ ) is useful to know, its value in DPK studies resides in the fact that it permits the normalisation of all data (from different subjects, obtained at different times), in terms of  $h/H$  or  $g/G$ , and enables direct comparison of different formulations and their equivalence (or not) to be established.

Figure 4 presents the  $h/H$  and  $g/G$  values determined for 388 tapes. These measurements are significantly ( $p < 0.0001$ ) and positively correlated (Spearman correlation coefficient ( $r_s$ )=0.99). This result strongly supports the interchangeability of  $h/H$  and  $g/G$  values and that the imaging method may

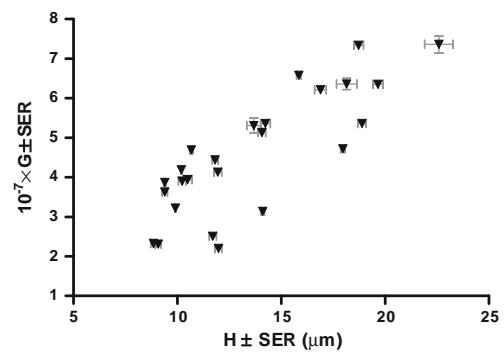


**Fig. 2** Correlation between the SC thickness estimates,  $H$  and  $G$ , with their respective standard errors of the regression (SER), for 25 experimental sites. Correlation is significant ( $p < 0.0001$ ) with a 2-tailed Gaussian approximation; Spearman correlation coefficient,  $r_s=0.80$ .

be confidently used to determine the relative position reached within the SC in DPK studies.

As the  $h/H$  and  $g/G$  values are cumulative and not independent, Eqs. 5 and 6 were used to calculate, for each tape ( $i$ ) respectively, the absolute normalised thickness ( $ANT_i$ ) and absolute normalised integrated pixel density ( $ANG_i$ ); the results are in Fig. 5. There was no statistical difference between  $ANT_i$  and  $ANG_i$  values (paired 2-tail T-test,  $p=0.98$ ), although the more extreme values of  $ANT_i$ , and their greater standard deviation (0.019 versus 0.015 for  $ANG_i$ ), are consistent with the better precision of the imaging method as recently reported (14). Further, the narrower spread of the  $ANG_i$  values (0.041–0.072; average= $0.057 \pm 0.015$ ), compared to that of  $ANT_i$  (0.038–0.075; average= $0.057 \pm 0.019$ ), suggests that the imaging approach may have a higher sensitivity to distinguish between the subtly different amounts of SC on the tape-strips (Fig. 5).

### Estimation of Drug Concentration Profiles

Subsequently, in a brief, proof-of-concept study, two acyclovir creams were compared. SC quantities on all tape-strips from

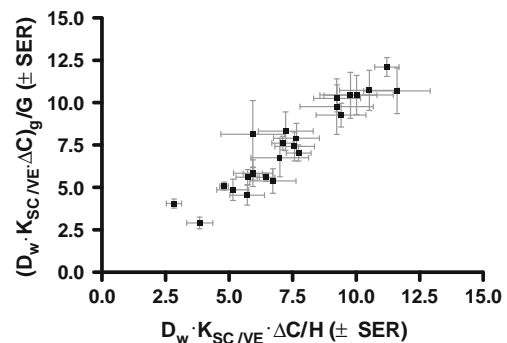


**Fig. 3** Comparison of the (normalised)  $D_w \cdot K_{SC/NE} \cdot \Delta C/H$  and  $(D_w \cdot K_{SC/NE} \cdot \Delta C)_g/G$  estimates (with their respective SER) for 25 different sites; a significant correlation ( $\alpha=0.05$ ) is found with a 2-tail non-parametric test ( $p < 0.0001$ ,  $r_s=0.93$ ).

**Table I** Inter-Subject Variability in H and G When Multiple Sites Were Examined on the Same Arm on the Same Day

	Subject 1 (n=4)		Subject 2 (n=3)		Subject 3 (n=4)		Subject 4 (n=5)	
	H ( $\mu\text{m}$ )	$10^{-7} \times G$	H ( $\mu\text{m}$ )	$10^{-7} \times G$	H ( $\mu\text{m}$ )	$10^{-7} \times G$	H ( $\mu\text{m}$ )	$10^{-7} \times G$
Average	10.8	4.2	19.2	6.6	10.0	3.7	16.1	5.5
SD	1.3	0.2	3.0	0.6	0.5	0.3	2.9	0.5
RSD (%)	11.6	5.6	15.6	9.4	4.7	9.0	18.1	8.8

each application site were assessed both gravimetrically and by the imaging method. Two drug-permeation profiles were thereby produced, allowing differences (a) between the gravimetric and imaging profiles, and (b) between the acyclovir formulations, to be considered as shown in Figs. 6 and 7. To facilitate the comparisons, the 'normalised concentration of drug in the SC' was calculated, using Eqs. 7 and 8.

The resulting DPK data from the skin sites treated with the Zovirax and Pliva creams are shown in Figs. 6 and 7, respectively, and the normalised profiles generally overlap rather well. This means that measurements derived from the imaging method provide a perfectly usable relative assessment of the performance of the two topical products, with no need for explicit knowledge of the absolute depth of drug penetration into the SC.<sup>1</sup>

The normalised concentration profiles were fitted to Eqs. 9 and 10 and the ACV diffusivity parameter in the SC ( $D/H^2$ ), and the normalised partition coefficients ( $K_m/R_m$  and  $K_g/R_g$ , respectively), were determined (Table II). As may be anticipated from the superposition of the drug permeation profiles in Figs. 6 and 7, there was no significant difference between the results derived from the gravimetric and imaging approaches (2-tail paired non-parametric t-test,  $p > 0.05$ ).

Estimations of the average ACV concentrations in the SC,  $R_m$  (Eq. 7) and  $R_g$  (Eq. 8) are also presented in Table II. The latter allows  $K_g/R_g$  to be converted into a true vehicle-SC partition coefficient,  $K_m$ . Notably, this will permit future DPK evaluations of formulations undertaken with the imaging method to be directly compared with previously studied products, for which the SC per tape was measured gravimetrically.

The SC-vehicle partition coefficient values for Zovirax were largely reproducible, with  $K_m$  varying between 3.7 and 6.4, and  $K_g$  from  $3.1 \times 10^{-5}$  to  $9.5 \times 10^{-5}$  over the four sites. The  $D/H^2$  values were consistently between 0.02 and  $0.04 \text{ h}^{-1}$  for both SC quantification methods. The higher  $D/H^2$  value observed for Subject 5 at Zovirax site 1 (Table II) is due to a 'spike' in the ACV concentration at

$h/H$  or  $g/G \sim 0.6$  (see Fig. 6a) and is most likely due to an unexplained contamination.

## DISCUSSION

In the first series of experiments reported here, SC on tapes from 25 untreated skin sites was quantified gravimetrically and with a novel imaging method. The former approach is well established in DPK studies (12–20) and, when used in conjunction with measurements of TEWL, the total SC thickness may be estimated (23). The latter technique, which is based on the determination of cumulative greyscale values of successive tapes (24), has also been demonstrated to provide an assessment of SC thickness that correlates well with the gravimetric method. Furthermore, the intra-subject variability associated with results from the imaging technique was found to be smaller due, it is believed, to the improved signal-to-noise ratio of the approach.

The interpretation of drug concentration profiles across the skin (12–20) has been facilitated by analyzing the data as a function of the *normalised* depth of penetration into the barrier (as expressed in this paper by  $h/H$ ). This permits results from different subjects with different absolute SC thicknesses to be objectively compared. The data derived for the imaging evaluation of SC amounts removed per tape-strip can also provide corresponding, normalised quantification of relative position within the membrane (described by  $g/G$  in this work). The correlation between  $h/H$  and  $g/G$  (and that between  $D_w \cdot K_{SC}/V_E \cdot \Delta C/H$  and

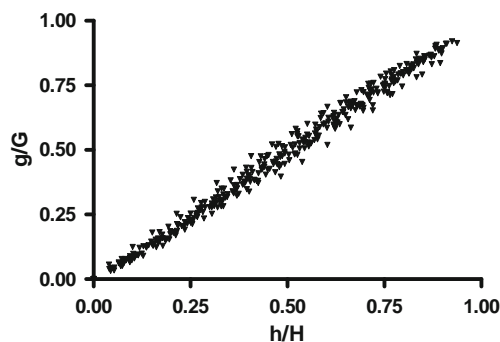
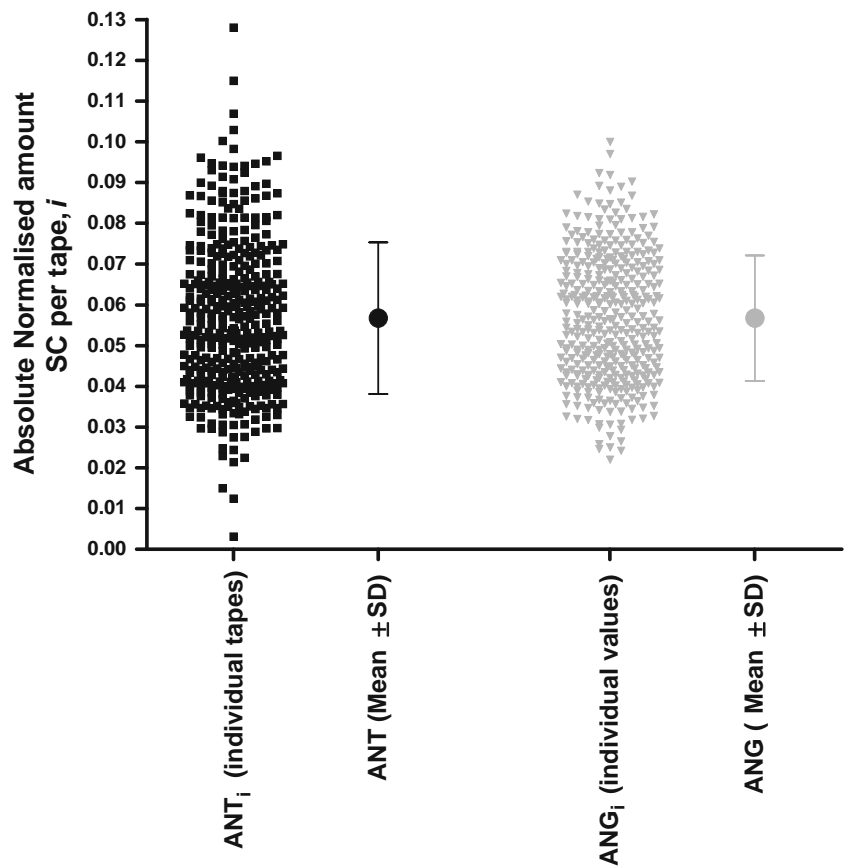


**Fig. 4** Correlation between the  $h/H$  and  $g/G$  values determined from tape-stripping 25 skin sites ( $n=388$  tape-strips collected from 8 volunteers). The correlation (2-tail) is significant ( $p < 0.0001$ ), with  $r_s=0.99$ .

<sup>1</sup> It should be noted, however, that application of Pliva cream to site 2 of Subject 5 caused significant SC disruption, resulting in visible 'clumps' of the barrier being removed, and a resulting high concentration of drug, on certain tape-strips (see, for instance, the result for tape 3 from this site in Fig. 7b). It was not possible, therefore, to further analyse this profile.

**Fig. 5** Absolute normalised thickness ( $ANT_i$ , ■, Eq. 5) and absolute normalised integrated pixel density ( $ANG_i$ , ▼, Eq. 6) values for each tape,  $i$  ( $n=388$ ); no significant difference between the  $ANT$  and  $ANG$  values (paired 2-tail t-test ( $p=0.98$ ; pairing was effective ( $p<0.0001$ )). Means (●) and standard deviations are also presented for each method.



$(D_w \cdot K_{SC/VE} \cdot \Delta C)_g / G$ ) is shown to be excellent, meaning that the normalised SC position derived from imaging can be used in place of that obtained from the much more labour-intensive gravimetric approach. The advantage of the greyscale method, relative to the established procedure, is further reinforced by its overall better precision (fewer outliers)

and sensitivity (wider dynamic range) reflected in the absolute normalised SC amount per tape.

A proof-of-concept DPK study was then undertaken to test whether the imaging method for SC quantification could be used in the comparison of two topical formulations of acyclovir. SC amounts per tape-strip were also determined

**Fig. 6** DPK profiles of acyclovir after application of Zovirax cream. The normalised concentrations on the y-axes were determined using Eqs. 7 and 8, respectively, for SC amounts per tape determined either gravimetrically ( $\square$ ) or by the imaging method ( $\blacklozenge$ ). Fitting the data to Eqs. 9 (—) and 10 (---) is also shown. (a, b) Subject 5, sites 1 and 2, respectively. (c, d) Subject 6, sites 1 and 2, respectively.

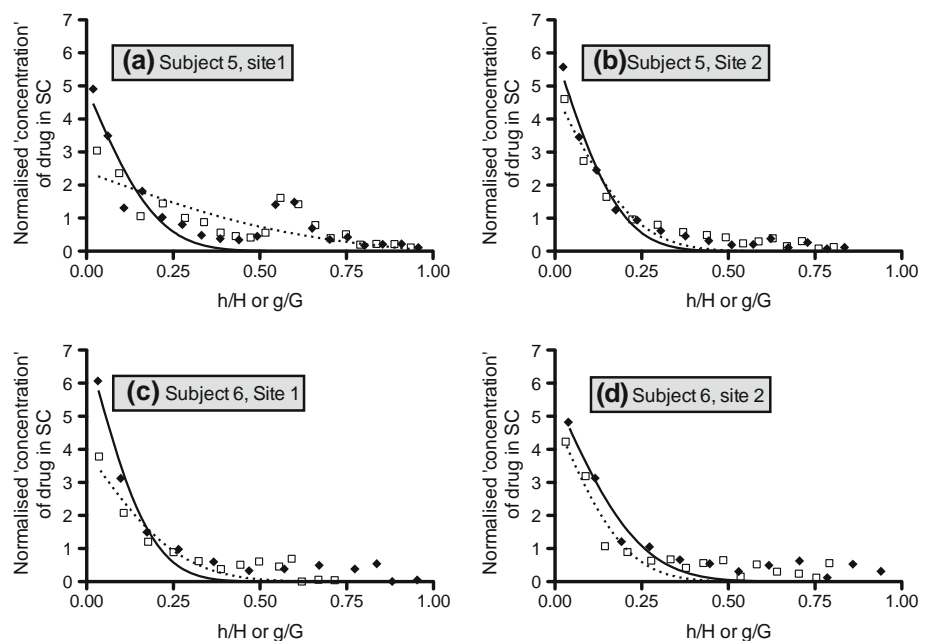
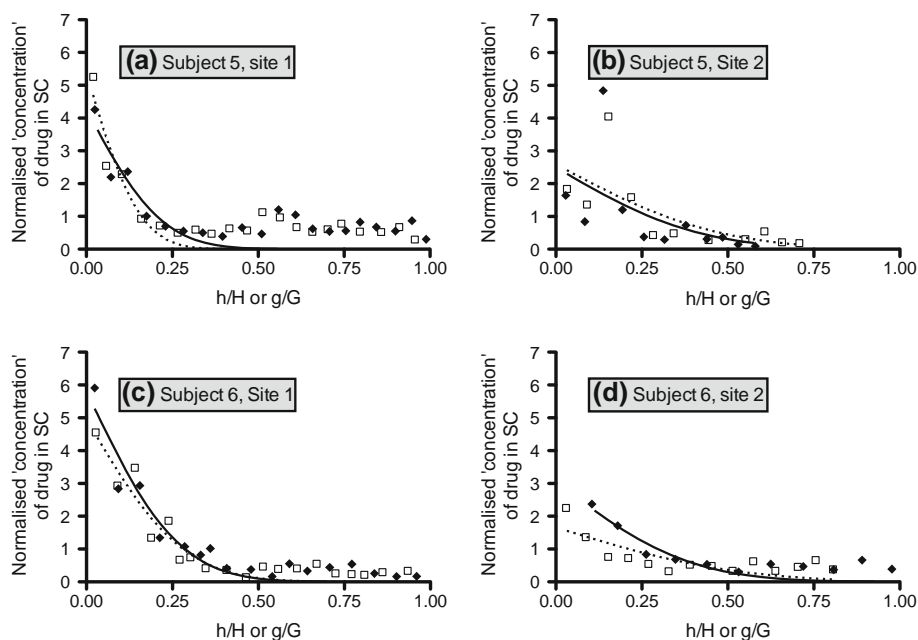




**Fig. 7** DPK profiles of acyclovir after application of Pliva cream. The normalised concentrations on the y-axes were determined using Eqs. 7 and 8, respectively, for SC amounts per tape determined either gravimetrically ( $\square$ ) or by the imaging method ( $\blacklozenge$ ). Fitting the data to Eqs. 9 (—) and 10 (---) is also shown. (a) Subject 5, site 1. (c, d) Subject 6, sites 1 and 2, respectively. (b) Subject 5, site 2 shown for information only; evidence of SC disruption by Pliva cream at this site, with clumps of SC removed on tapes, resulting in high concentration of drug in SC on tape 3.



gravimetrically to provide validation of the imaging approach. It was first established that normalisation of the penetration depth (by  $h/H$  or  $g/G$ ) led to superimposable acyclovir concentration profiles across the SC. Equally, when these profiles were fitted to the appropriate solutions of Fick's 2nd law of diffusion, there were no significant differences in the derived diffusion and partitioning parameters. It follows that further assessment of DPK characteristics using the imaging technique will be comparable with previous results obtained from gravimetric measurement of SC position.

The derived partition coefficients determined in this investigation for acyclovir are mostly within an order of magnitude of those reported in the literature (13,16,17,19) for other drugs of markedly different physicochemical properties. These observations imply that the drug concentration

in the SC at the surface of the barrier is approximately equal to that in the vehicle. One interpretation for this (apparent) coincidence is that residual formulation remains on the skin surface, or in the skin furrows (15), after the skin has been cleaned and before tape stripping commences. Alternatively, it may be hypothesised that the drug, and key formulation excipients in which the drug is soluble, enter the SC as a "unit", and only separate from one another deeper within the barrier. There is some evidence for this idea in recent publications (18,28): first, the uptake of ibuprofen into the SC from vehicles, in which the drug is present at the same (maximum) thermodynamic activity, is not constant but rather increases with the percentage of cosolvent (propylene glycol) in the formulation (18); second, the more rapid, subsequent diffusion of propylene glycol, relative to ibuprofen, through

**Table II** Estimates ( $\pm$  Standard Error) of  $K$  and  $D/H^2$  from Fick's 2nd Law, for Zovirax and Pliva Formulations, with SC Measured Using Gravimetric and Imaging Techniques (Eqs. 9 and 10, Respectively)

Subject	Site	$R_m^a$	$10^5 \times R_g^a$	Normalised data		$(D/H^2)_{\text{mass}} (h^{-1})^{bc}$	$(D/H^2)_{\text{greyscale}} (h^{-1})^{bc}$	$K_m$	$10^5 \times K_g$
				$K_m/R_m^{bc}$	$K_g/R_g^{bc}$				
5	Zov. 1	1.6	1.0	$2.4 \pm 0.3$	$4.9 \pm 0.7$	$0.24 \pm 0.09$	$0.03 \pm 0.01$	$3.7 \pm 0.5$	$4.7 \pm 0.6$
	Zov. 2	0.9	0.5	$4.8 \pm 0.4$	$6.0 \pm 0.3$	$0.03 \pm 0.01$	$0.02 \pm 0.00$	$4.1 \pm 0.3$	$3.1 \pm 0.2$
6	Zov. 1	1.6	1.3	$4.0 \pm 0.4$	$7.1 \pm 0.5$	$0.04 \pm 0.01$	$0.02 \pm 0.00$	$6.4 \pm 0.7$	$9.5 \pm 0.8$
	Zov. 2	0.9	0.8	$4.9 \pm 0.5$	$5.6 \pm 0.5$	$0.03 \pm 0.01$	$0.04 \pm 0.01$	$4.6 \pm 0.5$	$4.4 \pm 0.4$
5	Pliva 1	1.2	0.7	$5.4 \pm 0.7$	$4.3 \pm 0.7$	$0.01 \pm 0.01$	$0.03 \pm 0.01$	$6.3 \pm 0.9$	$2.9 \pm 0.5$
6	Pliva 1	2.4	2.4	$5.0 \pm 0.4$	$5.8 \pm 0.4$	$0.05 \pm 0.01$	$0.04 \pm 0.01$	$11.8 \pm 0.9$	$13.8 \pm 1.1$
	Pliva 2	1.8	1.5	$1.7 \pm 0.3$	$2.8 \pm 0.5$	$0.17 \pm 0.07$	$0.12 \pm 0.04$	$2.9 \pm 0.5$	$4.2 \pm 0.7$

<sup>a</sup>  $R_m$  and  $R_g$  defined in Eqs. 7 and 8, respectively

<sup>b</sup> Derived from fitting the normalised DPK data to Eqs. 9 and 10

<sup>c</sup> No statistical difference between the values derived from the gravimetric and imaging methods [2-tail paired non-parametric t-test,  $p > 0.05$ ]

the SC significantly impacts on drug clearance from the barrier (28) and has led its precipitation being observed in the surface layers (29) as the local concentration increases above the solubility. It follows that the assessment of bioequivalence between formulations must also consider carefully the potential impact of differences in the nature and quantity of the excipients present. As a sensible starting point, for example, one might explore the use of the new imaging tools now being used in DPK studies (24,29) to examine acyclovir formulations, which have been shown in earlier research to be clearly bio-inequivalent (30).

## CONCLUSIONS

The mean cumulative greyscale values, derived from the imaging method, may be used instead of cumulative thickness estimates derived from the gravimetric approach (a) to provide direct measurement of the relative depth reached within the SC with each tape, (b) to estimate total SC thickness, and (c) to evaluate DPK parameters. The cumulative greyscale values are generally more precise and sensitive, and have less intra-subject variability. In addition, the imaging method is faster and simpler, has a higher signal-to-noise ratio, makes use of all the SC collected on a tape-strip and provides a permanent, digital record of the tape's image (24). Overall, therefore, the imaging method represents an experimental strategy with the potential to further enhance the value of SC tape stripping as a valid and informative approach for the assessment of bioequivalence between topical medicines.

## ACKNOWLEDGMENTS

LMR thanks the University of Bath for the award of a PhD studentship.

## REFERENCES

1. Wiedersberg S, Nicoli S. Skin permeation assessment: tape stripping. In: Benson HAE, Watkinson AC, editors. Topical and transdermal drug delivery: principles and practice. Hoboken: John Wiley and Sons Inc; 2012. p. 109–30.
2. Pershing LK, Nelson JL, Corlett JL, Shrivastava SP, Hare DB, Shah VP. Assessment of dermatopharmacokinetic approach in the bioequivalence determination of topical tretinoin gel products. *J Am Acad Dermatol*. 2003;48:740–51.
3. Pershing LK, Bakhtian S, Poncelet CE, Corlett JL, Shah VP. Comparison of skin stripping, *in vitro* release, and skin blanching response methods to measure dose response and similarity of triamcinolone acetonide cream strengths from two manufactured sources. *J Pharm Sci*. 2002;91:1312–24.
4. Lademann J, Jacobi U, Surber C, Weigmann H-J, Fluhr JW. The tape stripping procedure-evaluation of some critical parameters. *Eur J Pharm Biopharm*. 2009;72:317–23.
5. Boix-Montanes A. Relevance of equivalence assessment of topical products based on the dermatopharmacokinetics approach. *Eur J Pharm Sci*. 2011;42:173–9.
6. Rougier A, Lotte C, Maibach HI. *In vivo* percutaneous penetration of some organic compounds related to anatomic site in humans: predictive assessment by the stripping method. *J Pharm Sci*. 1987;76:451–4.
7. Weigmann H-J, Lademann J, Meffert H, Schaefer H, Sterry W. Determination of the horny layer profile by tape stripping in combination with optical spectroscopy in the visible range as a prerequisite to quantify percutaneous absorption. *Skin Pharmacol Appl Skin Physiol*. 1999;12:34–45.
8. Lindemann U, Weigmann H-J, Schaefer H, Sterry W, Lademann J. Evaluation of the pseudo-absorption method to quantify human stratum corneum removed by tape stripping using the protein absorption. *Skin Pharmacol Physiol*. 2003;16:228–36.
9. Weigmann H-J, Lindemann U, Antoniou C, Tsirikas GN, Stratigos AI, Katsambas A, Sterry W, Lademann J. UV/VIS absorbance allows rapid, accurate, and reproducible mass determination of corneocytes removed by tape stripping. *Skin Pharmacol Appl Skin Physiol*. 2003;16:217–27.
10. Au WL, Skinner M, Kanfer I. Comparison of tape stripping with the human skin blanching assay for the bioequivalence assessment of topical clobetasol propionate formulations. *J Pharm Pharm Sci*. 2010;13:11–20.
11. Parfitt NR, Skinner MF, Bon C, Kanfer I. Bioequivalence of topical clotrimazole formulations: an improved tape stripping method. *J Pharm Pharm Sci*. 2011;14:347–57.
12. Herkenne C, Naik A, Kalia YN, Hadgraft J, Guy RH. Pig ear skin *ex vivo* as a model for *in vivo* dermatopharmacokinetic studies in man. *Pharm Res*. 2006;23:1850–6.
13. Alberti I, Kalia YN, Naik A, Guy RH. Assessment and prediction of the cutaneous bioavailability of topical terbinafine, *in vivo*, in man. *Pharm Res*. 2001;18:1472–5.
14. Alberti I, Kalia YN, Naik A, Bonny JD, Guy RH. *In vivo* assessment of enhanced topical delivery of terbinafine to human stratum corneum. *J Control Release*. 2001;71:319–27.
15. Wiedersberg S, Leopold CS, Guy RH. Dermatopharmacokinetics of betamethasone 17-valerate: influence of formulation viscosity and skin surface cleaning procedure. *Eur J Pharm Biopharm*. 2009;71:362–6.
16. Herkenne C, Naik A, Kalia YN, Hadgraft J, Guy RH. Dermatopharmacokinetic prediction of topical drug bioavailability *in vivo*. *J Invest Dermatol*. 2007;127:887–94.
17. Herkenne C, Naik A, Kalia YN, Hadgraft J, Guy RH. Ibuprofen transport into and through skin from topical formulations: *in vitro-in vivo* comparison. *J Invest Dermatol*. 2007;127:135–42.
18. Herkenne C, Naik A, Kalia YN, Hadgraft J, Guy RH. Effect of propylene glycol on ibuprofen absorption into human skin *in vivo*. *J Pharm Sci*. 2008;97:185–97.
19. Wiedersberg S, Naik A, Leopold CS, Guy RH. Pharmacodynamics and dermatopharmacokinetics of betamethasone 17-valerate: assessment of topical bioavailability. *Br J Dermatol*. 2009;160:676–86.
20. Alberti I, Kalia YN, Naik A, Bonny J, Guy RH. Effect of ethanol and isopropyl myristate on the availability of topical terbinafine in human stratum corneum, *in vivo*. *Int J Pharm*. 2001;219:11–9.
21. Anderson RL, Cassidy JM. Variations in physical dimensions and chemical composition of human stratum corneum. *J Invest Dermatol*. 1973;61:30–2.
22. Kalia YN, Pirot F, Guy RH. Homogeneous transport in a heterogeneous membrane: water diffusion across human stratum corneum *in vivo*. *Biophys J*. 1996;71:2692–700.

23. Russell LM, Wiedersberg S, Delgado-Charro MB. The determination of stratum corneum thickness - an alternative approach. *Eur J Pharm Biopharm.* 2008;69:861–70.
24. Russell LM, Guy RH. Novel imaging method to quantify stratum corneum in dermatopharmacokinetic studies. *Pharm Res.* 2012;in press. doi: [10.1007/s11095-012-0764-y](https://doi.org/10.1007/s11095-012-0764-y).
25. Denda M, Wood LC, Emami S, Calhoun C, Brown BE, Elias PM, Feingold KR. The epidermal hyperplasia associated with repeated barrier disruption by acetone treatment or tape stripping cannot be attributed to increased water loss. *Arch Dermatol Res.* 1996;288:230–8.
26. Eriksson G, Lamke LO. Regeneration of human epidermal surface and water barrier function after stripping. A combined study with electron microscopy and measurement of evaporative loss. *Acta Derm Venereol.* 1971;51:169–78.
27. Frodinand T, Skogh M. Measurement of transepidermal water loss using an evaporimeter to follow the restitution of the barrier layer of human epidermis after stripping the stratum corneum. *Acta Derm Venereol.* 1984;64:537–40.
28. Nicoli S, Bunge AL, Delgado-Charro MB, Guy RH. Dermatopharmacokinetics: factors influencing drug clearance from the stratum corneum. *Pharm Res.* 2009;26:865–71.
29. Saar BG, Contreras-Rojas LR, Xie XS, Guy RH. Imaging drug delivery to skin with stimulated Raman scattering microscopy. *Mol Pharmaceut.* 2011;8:969–75.
30. Trotter L, Owen H, Holme P, Heylings J, Collin IP, Breen AP, Siyad MN, Nandra RS, Davis AF. Are all aciclovir cream formulations bioequivalent? *Int J Pharm.* 2005;304:63–71.